uclan
University of Central Lancashire

Article

Reversible Reaction of CO2 with Superbasic Ionic Liquid [P66614][benzim] Studied with in Situ Photoelectron Spectroscopy

Henderson, Zoe, Thomas, Andrew G., Wagstaffe, Michael, Taylor, S. F. Rebecca, Hardacre, Christopher and Syres, Karen

Available at http://clok.uclan.ac.uk/27895/

It is advisable to refer to the publisher's version if you intend to cite from the work.
http://dx.doi.org/10.1021/acs.jpcc.8b11670

For more information about UCLan's research in this area go to
http://www.uclan.ac.uk/researchgroups/ and search for <name of research Group>.

For information about Research generally at UCLan please go to
http://www.uclan.ac.uk/research/

CLoK
Central Lancashire online Knowledge
www.clok.uclan.ac.uk

CLoK
University of Central Lancashire's Institutional Repository

Reversible Reaction of CO$_2$ with Superbasic Ionic Liquid [P$_{66614}$][benzim] Studied with *In Situ* Photoelectron Spectroscopy

Zoë Henderson[†], Andrew G. Thomas[‡]*, Michael Wagstaffe[§⊥], S. F. Rebecca Taylor[∥], Christopher Hardacre[∥], Karen L. Syres[†]*

[†]   Jeremiah Horrocks Institute for Mathematics, Physics and Astronomy, University of Central Lancashire, Fylde Road, Preston, PR1 2HE, United Kingdom

[‡]   School of Materials and Photon Science Institute, University of Manchester, Oxford Road, Manchester, M13 9PL, United Kingdom

[§]   School of Physics and Astronomy, University of Manchester, Oxford Road, Manchester, M13 9PL, United Kingdom

[∥]   School of Chemical Engineering and Analytical Science, University of Manchester, Oxford Road, Manchester, M13 9PL, United Kingdom

ABSTRACT

Ionic liquids (ILs) are of significant interest as CO_2 capture agents, and one subgroup of ILs that has shown particular promise is that of superbasic ILs. They can absorb large quantities of CO_2 in the dry state, but some will have a diminished CO_2 capacity when pre-wetted. In the work presented here, the superbasic IL trihexyl-tetradecylphosphonium benzimidazolide, or [P_{66614}][benzim], was exposed to 3 mbar CO_2, 2 mbar H_2O vapor, and a $CO_2 + H_2O$ gas mixture; and investigated using near-ambient pressure X-ray photoelectron spectroscopy. The results show that the IL reacts with CO_2 to form carbamate, and that the reaction is reversible through reduction of the surrounding gas pressure. Regardless of whether the IL was exposed to CO_2 or H_2O vapor first, the presence of H_2O under these experimental conditions does not significantly hinder the IL's ability to absorb and react with CO_2. Furthermore, the IL appears to preferentially react with CO_2 over H_2O vapor.

INTRODUCTION

International commitments to a reduction in global CO_2 emissions could be in part met by CO_2 sequestration and storage, or utilization[1-3]. As a result, there is a pressing desire to identify stable, practical and economically viable methods to achieve this. Currently, the most widely used industrial solution is monoethanolamine (MEA)[4-5]. When MEA reacts with CO_2, it forms a carbamate species (COO^-) and a protonated MEA species (see Scheme 1). MEA is relatively cheap as a bulk solvent, but is extremely corrosive and requires a relatively large amount of energy to regenerate it following CO_2 capture[6]. Both of these factors contribute to increased costs where CO_2 is required to be removed.

Ionic liquids (ILs) have been widely investigated as potential CO_2 capture agents due to their advantageous properties, including ultra-low vapor pressures and excellent thermal stability. They are relatively easy to handle, and the regeneration of ILs after CO_2 capture is a relatively low energy process[6-7]. ILs can capture CO_2 via chemisorption or physisorption, and in previous years, attempts to improve the CO_2 capture capabilities of ILs have been successful with the addition of amine functional groups[8]. These react with CO_2 in much the same way as MEA (see Scheme 1). However, a problematic repercussion of CO_2 absorption in amine-functionalized ILs is an increase in their viscosity, which tends to inhibit further CO_2 absorption.

Current research also suggests that the presence of water in the gas stream can assist or hinder the ability of an IL to capture CO_2, depending on the constituent ions of the IL and the concentration of water. While the addition of water in amine-functionalized ILs reduces their viscosity, it also results in a decrease in CO_2 uptake[9]. The decrease in CO_2 uptake is attributed to protonation of the pyridine-like N group, which reduces the number of available sites for CO_2 to chemically bind[9]. The addition of small amounts of water has shown to improve the CO_2 capture

capabilities of some ILs. Phenolate-based ILs, for example, capture CO_2 through chemisorption, and the addition of 2 wt% H_2O almost doubled the molar CO_2 absorption[10]. For acetate-based ILs, which capture CO_2 through physisorption, the molar absorption increased eightfold with the addition of 0.35 molar fraction of H_2O[11].

In recent years, so-called superbasic ILs (SBIL) have attracted particular interest. These ILs consist of an imidazolide anion (a deprotonated and negatively charged aromatic ion). Reaction with CO_2 leads to the exothermic formation of carbamate at one or more of the deprotonated amine sites[6, 12]. Studies of superbasic ILs by various groups have shown an excellent capacity for CO_2 capture, with molar ratios (n_x) of up to 1.6:1 (n_{CO2}:n_{IL})[6]. In addition, these superbasic ILs do not undergo a large increase in viscosity upon CO_2 saturation, which makes them potentially useful in large-scale applications. An experimental and theoretical study of superbasic ILs showed that the IL, trihexyl-tetradecylphosphonium benzimidazolide ([P_{66614}][benzim] - see Figure 1), was able to absorb equimolar quantities of CO_2 in the dry state, but exhibited a reduced capacity for CO2 absorption if the IL was pre-wetted[6, 12]. This could be problematic if they are to be considered for CO_2 capture on an industrial scale, since industrial flue gases consist of a complex mixture of gas molecules, including CO_2 and H_2O.

X-ray photoelectron spectroscopy (XPS) has been a useful tool in the analysis of surface reactions, and surface electronic structure of solids for many years[13-14]. The extremely low vapor pressure of ILs has also meant that in recent years studies of liquid surfaces have been possible[15-18]. Interactions between gases and ILs have been studied using XPS, but at low temperatures. The gas and the IL need to be cooled together (which forms a glassy structure), then gently heated to monitor gas desorption from the IL[19]. This process is necessary because, at the extremely low pressures required for XPS, gases often do not remain trapped or ad/absorbed in

any appreciable amount at ambient temperatures. Rivera-Rubero and Baldelli, for example, showed that water can be removed from the IL 1-butyl-3-methylimidazolium tetrafluoroborate ($[C_4C_1Im][BF_4]$) at pressures of $<1\times10^{-5}$ mbar at room temperature[20]. The recent availability of near-ambient pressure XPS (NAPXPS) has opened up the possibility of measurements of liquid surfaces in gas pressures of up to a few tens of mbar[4, 8, 21-23]. In our own work[24] and in work of groups such as the Newberg group[25-27], NAPXPS has allowed for surface-sensitive studies of the interactions between gas molecules and ILs. Herein, we examine the reaction of the superbasic IL, $[P_{66614}][benzim]$, with CO_2, H_2O and two mixed CO_2/H_2O vapor regimes using NAPXPS.

EXPERIMENTAL SECTION

The SBIL, $[P_{66614}][benzim]$ was prepared using a two-step synthesis, described previously[6]. The IL was dried under high vacuum (0.01 mbar at 50°C for 72 hours) and then transferred to a vial sealed with a rubber septum in a dry argon-filled glovebox prior to use. Around 0.5 ml of IL was deposited dropwise by syringe onto a Ta sample plate under ambient laboratory conditions. The plate was transferred to a vacuum load lock and the load lock pumped down and left to reach $<1\times10^{-6}$ mbar before transferring to the analysis chamber. During the preparation process, the sample was exposed to ambient lab atmosphere for around 5 minutes.

XPS analysis was carried out in a custom-built SPECS system equipped with a near-ambient pressure (NAP) cell, monochromated Al K_α X-ray source and SPECS Phoibos NAP150 hemispherical analyzer. CO_2 (CK Gases, purity 99.9995%) was further purified by passing it through a scrubber (SAES Microtorr) to remove trace impurities, particularly of CO. Doubly distilled water was purified by repeated freeze-thaw-pump cycles until no gas bubbles were observed in the water under a vacuum of 1×10^{-6} mbar. Spectra were recorded with electron emission normal to the surface from the top edge of the IL film to minimize the possibility of

sample charging. Normal emission and grazing emission XPS measurements were carried out in ultra-high vacuum (UHV) conditions (at a pressure of approximately 10^{-9} mbar; see Supporting Information (SI)) before being transferred to the NAP cell. NAPXPS measurements were carried out over seven stages in the NAP cell, as outlined in Scheme 2. During Stage 1, measurements were recorded from the unexposed IL. In Stage 2, the IL was exposed to 0.5 mbar of CO_2. For Stage 3, the CO_2 was pumped out of the NAP cell and measurements were taken when the pressure had stabilized at approximately 10^{-8} mbar, i.e. the IL was under high-vacuum conditions once again. Measurements taken at Stages 1 through 3 were to determine whether or not the CO_2 capture by the IL was reversible through a pressure swing to reduced pressure. In the measurements taken after Stage 3, the IL is referred to as 'regenerated'. Stage 4 involved exposing the regenerated IL to 3 mbar of CO_2. In Stage 5, 2 mbar H_2O vapor was introduced into the NAP cell, creating the first mixed-gas regime. During Stage 6, the CO_2 flow was turned off, leaving the IL exposed only to 2 mbar of H_2O vapor and measurements were taken when the pressure in the NAP cell had stabilized at 2 mbar. For the final stage, Stage 7, 3 mbar of CO_2 was reintroduced into the system giving a total CO_2 and water pressure of 5 mbar for the second mixed-gas regime.
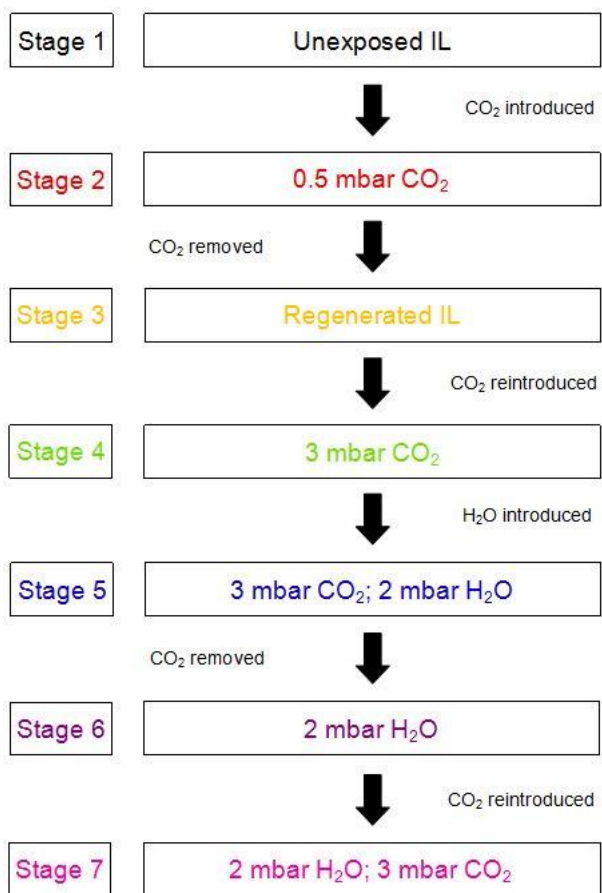
Scheme 1. Flow chart illustrating the stages of the experiment, numbered 1 to 7. The annotations between the stages describe which gases are introduced or removed. Measurements were taken at each stage.
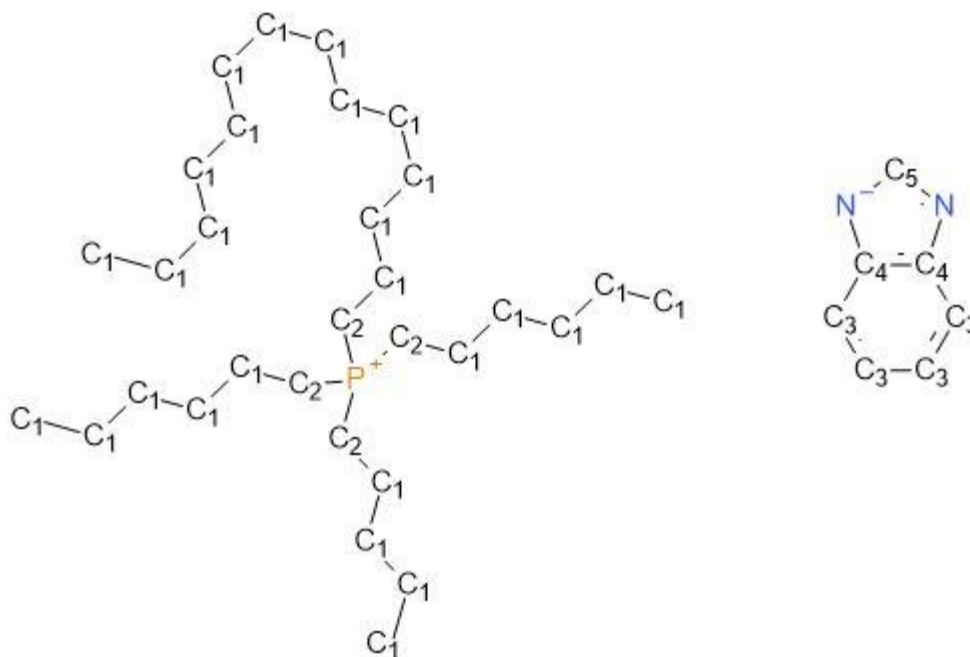
Figure 1. Ball-and-stick diagram showing the structure of the superbasic IL, trihexyl-tetradecylphosphonium benzimidazolide, or [P$_{66614}$][benzim]. The labels C^1 to C^5 highlight the different chemical environments of the carbon atoms present in the IL pair.

Each NAPXPS spectrum was recorded from a different position on the sample surface to avoid damage due to prolonged X-ray exposure. Each measurement took approximately one hour, and all measurements were taken at room temperature. Spectra are aligned on the binding energy (BE) scale relative to the aliphatic C 1s signal at 285.0 eV[28], with all BEs quoted to ± 0.1 eV. XPS core level peak fitting was carried out using CasaXPS software with a linear baseline and 70:30 Gaussian:Lorentzian lineshape[29].
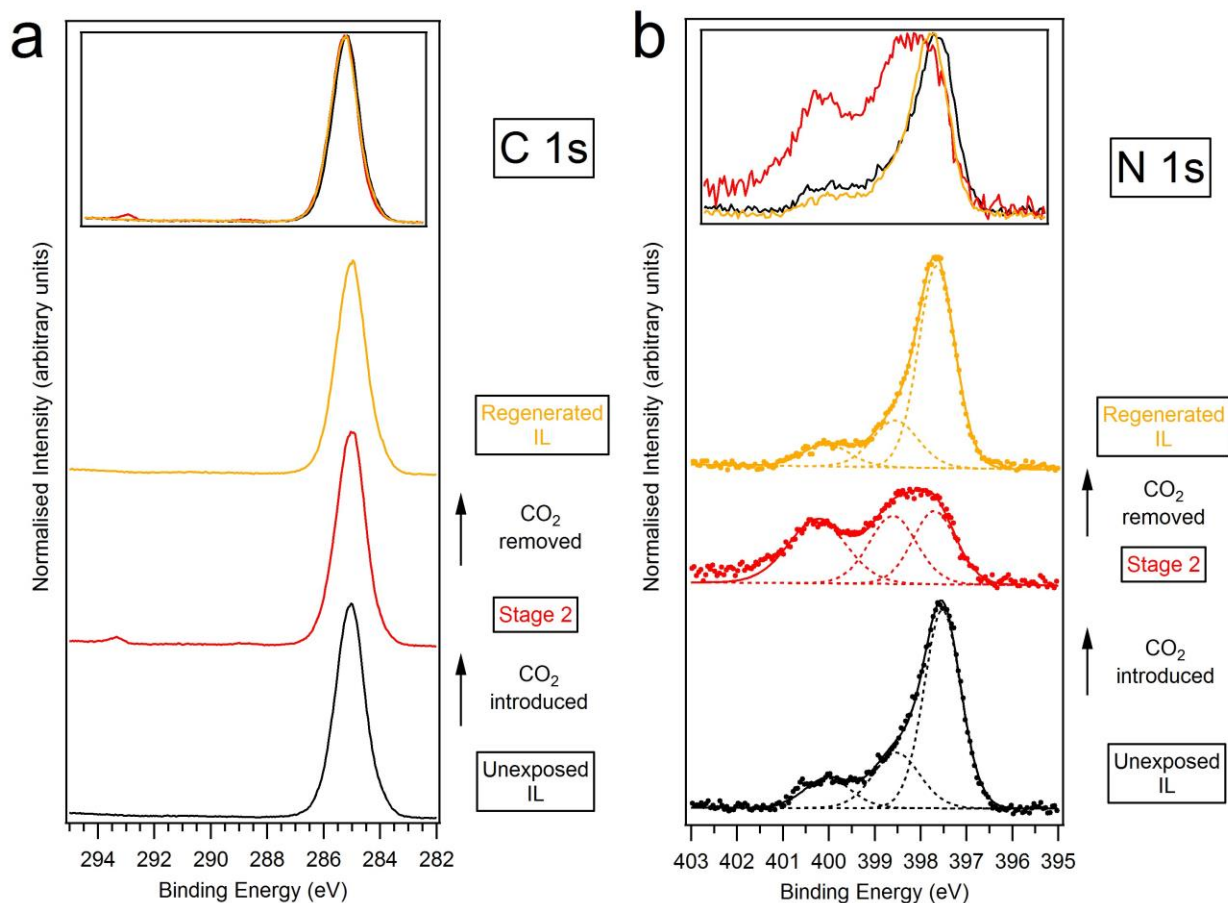
RESULTS AND DISCUSSION

Figure 2. The C 1s region (a), and N 1s region (b) of the unexposed IL (Stage 1, black line), of the IL during exposure to 0.5 mbar of CO_2 (Stage 2, red line), and of the regenerated IL (Stage 3, amber line). Each N 1s spectrum has been normalized to the total area, and each C 1s spectrum has been normalized to the IL carbon peak. The intensity of the spectra in the inset figures have been normalized to the most intense peak.

The C 1s and N 1s photoelectron spectra recorded from the IL during Stages 1 through 3 are shown in Figure 2, represented by the black, red and amber lines, respectively. In each region, the spectrum post-exposure is almost identical to the spectrum of the unexposed IL (see inset of Figure 2a and Figure 2b). This demonstrates that any interaction between the IL and CO_2 is reversible when the pressure in the NAP cell is reduced. Furthermore, these data suggest that the

IL can be largely regenerated through a reduction in pressure. The C 1s shows very little discernible change upon exposure to 0.5 mbar CO_2 and following regeneration by evacuation of the gas cell (see inset of Figure 2a). The N 1s, however, shows more significant changes in the presence of the gas with a broadening of the peak near 397.5 eV and the growth of a second feature at around 400 eV. The peak at 397.5 eV, which dominates the spectrum recorded from the unexposed film, is attributed to the nitrogen atoms of the [benzim]$^-$ anion (labelled N_{Im} in Figure 4). Due to resonance effects the two N atoms in the [benzim]$^-$ anion can be considered chemically equivalent[16-17]. The small feature at around 400 eV has been attributed to the presence of protonated benzimidazole. The growth of this peak and the associated broadening of the lower binding energy feature on exposure to CO_2, coupled with the loss of these features on removal of CO_2, indicate these features are associated with the interaction with CO_2. In order to investigate the origin of these features the regenerated IL was exposed to CO_2 and H_2O in stages as described above.
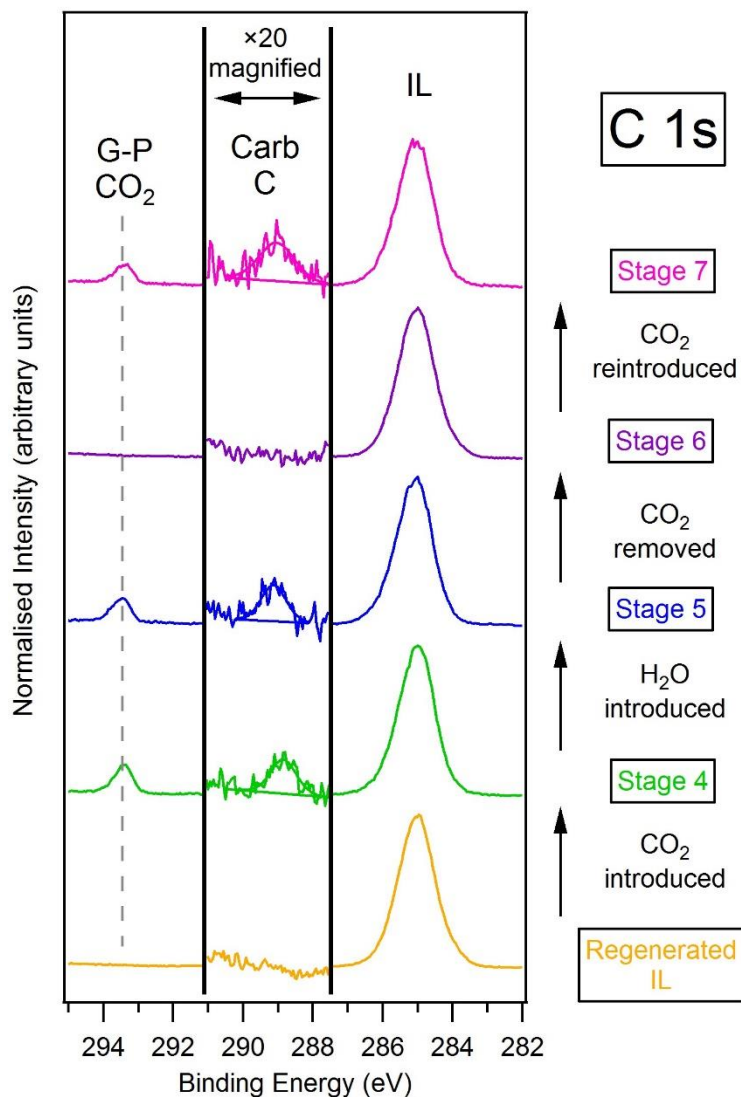
Figure 3. C 1s spectrum taken of the regenerated IL (Stage 3, amber line), of the IL during exposure to 3 mbar CO_2 (Stage 4, green line), during exposure to the first mixed-gas regime (Stage 5, blue line), during exposure to 2 mbar H_2O (Stage 6, violet line), and during exposure to the second mixed-gas regime (Stage 7, magenta line). The data between 291.0 eV and 287.5 eV is ×20 magnified. The term gas-phase is abbreviated to 'G-P', and carbamate is shortened to 'Carb'.

Figure 3 shows the C 1s spectra recorded through Stages 3 to 7. All of the C 1s spectra feature a strong, slightly asymmetric signal at 285.0 eV. This signal is attributed to the carbon atoms in [P_{66614}][benzim]. Blundell and Licence[28] studied other ILs with the same cation using XPS. They resolved the asymmetrical peak associated with the [P_{66614}]$^+$ cation into two components: one attributed to the hetero (C-P) carbon, and one attributed to the alkyl (C-C) carbon (the hetero carbons and alkyl carbons are labelled as C^2 and C^1 respectively in Figure 1). The C 1s signal in this work will consist of contributions from these carbon environments, in addition to contributions from the aromatic carbon species of the anion (labelled C^3 to C^5 in Figure 1). However, none of the contributions from either the cation or the anion have been fitted here, since fitting any components to this peak would be speculative at best given the broad nature of the peak. Upon exposure to 3 mbar CO_2 (Stage 4, represented by the green line), two more signals appear in the region. The peak at a BE of 293.4 eV is attributed to gas phase CO_2 and the peak observed at a BE of approximately 289.0 eV is attributed to carbamate formation[30]. These peaks do not change significantly in shape upon exposure to water during the first mixed-gas regime (Stage 5, represented by the blue line), but there is a slight upward shift in BE for the carbamate CO_2 peak from 288.8 eV to 289.1 eV. In numerous studies, the BE of peaks associated with ad/absorbed gas species tend to shift with increased coverage (in the case of adsorbates), or increased gas pressure[31-34]. Since the IL was subject to further CO_2 exposure during Stage 5, it is, therefore, likely that this shift is due to an increase in absorbed CO_2 in the IL. During Stage 6 (2 mbar H_2O vapor only, represented by the violet line), the signal attributed to carbamate CO_2 is no longer present, indicating desorption of CO_2 from the IL. When 3 mbar of CO_2 is then reintroduced into the NAP cell (Stage 7, represented by the magenta line), the

peak at ~289.0 eV returns, with a similar intensity to that seen in Stage 5. The peak assignments are summarized in Table 1.

Table 1. Binding energies and assignments of all peaks in the C 1s, O 1s, and N 1s regions throughout the experiment.

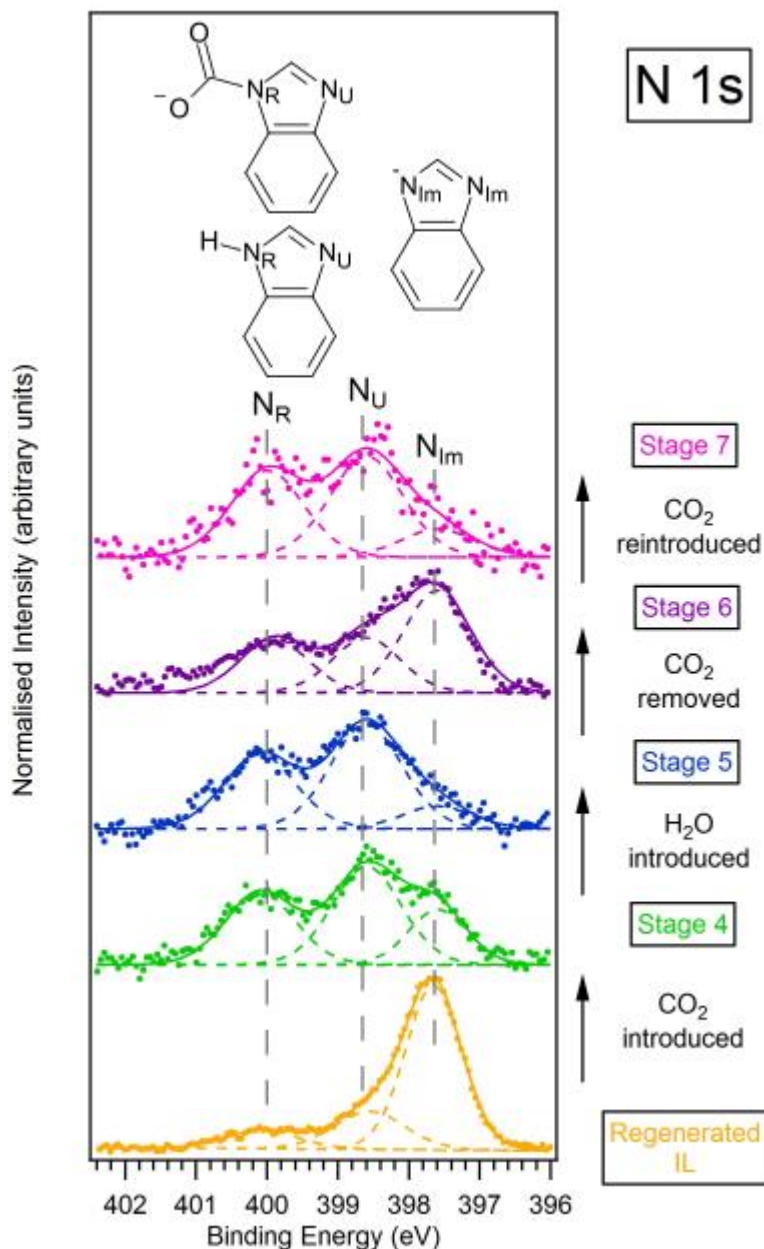| Region	Binding Energy (eV) (±0.1 eV)	Assignment
C 1s	285.0	IL C
	289.0	Carbamate C
	293.4	Gas-phase CO_2
N 1s	397.5	Imidazolide N
	398.5	Unreacted N
	400.0	Reacted N

Figure 4. N 1s spectrum taken of the regenerated IL (Stage 3, amber line), of the IL during exposure to 3 mbar CO_2 (Stage 4, green line), during exposure to the first mixed-gas regime (Stage 5, blue line), during exposure to 2 mbar H_2O (Stage 6, violet line), and during exposure to the second mixed-gas regime (Stage 7, magenta line). The label N_{Im} refers to the imidazolide N. The labels N_U and N_R refer to the unreacted and reacted N respectively. Each spectrum has been normalized to the total area of the region. Chemical structures of an ordinary [benzim]$^-$ anion

(with N atoms labelled N_{Im}) and reacted [benzim]⁻ anions (with N atoms labelled N_U and N_R) are featured above the spectra.

Figure 4 shows the N 1s spectrum through Stages 3 to 7 of the experiment. The spectrum of the regenerated IL (amber line) can be fitted with three peaks at binding energies of 397.5 eV, 398.5 eV and 400.0 eV. The peak at 397.5 eV is assigned to the imidazolide N atoms, as described above. The two peaks at higher BE are seen to increase in intensity when the IL is exposed to 3 mbar of CO_2 in Stage 4 (green line). They are, therefore, attributed to the reaction between the IL and CO_2. The peak at 400 eV is attributed to the formation of carbamate, and has been labelled N_R, to mean 'reacted' N. Once a [benzim]⁻ anion has reacted with CO_2, the N atoms in the anion can no longer be considered as chemically equivalent. The reaction of the imidazolide ion with CO_2 will also mean the two N atoms in the anion will have a different charge density and therefore a different BE. As a result, the signal at 398.5 eV is attributed to a BE shift in this 'unreacted' N atom in the [benzim]⁻ anion that has reacted with CO_2 (labelled N_U in Figure 4).

When 2 mbar of H_2O is introduced to create the first mixed-gas regime (Stage 5, blue line), the N_U and N_R peaks continue to increase in intensity. This is likely to be due to continued reaction with CO_2, reaction between the IL and H_2O, or a combination of both. Imidazolide-based anions react with water to form an imidazole (protonated imidazolide) and a hydroxide anion (OH⁻)[35] (see Scheme 3). This reaction is seen in ¹H NMR spectra of [P₆₆₆₁₄][benzim]/H_2O mixtures, manifesting as a downward chemical shift[6]. Morales-Gil *et al.*[36] reported that for mercaptobenzimidazole a BE difference of 1.6 eV between pyridine-like (N) and the pyrrole-like (NH) nitrogen atoms. This BE difference is consistent with the BE difference between our N_U

and N_R peaks. In addition, Tenney *et al.*[4] showed only a small shift of 0.3 eV BE between the carbamate N and protonated N in an XPS study of 3-amino-1-propanol and CO_2. Therefore, on exposure to water we attribute the additional intensity of the N_U and N_R peaks to unreacted (non-protonated) N and reacted (protonated) N, respectively, as a result of the reaction between the IL and H_2O. To clarify, the N_R peak is attributed to a combination of $N\text{-}COO^-$ and NH signals, and the N_U peak is attributed to the unreacted N atom in the ring of a 'reacted' anion.
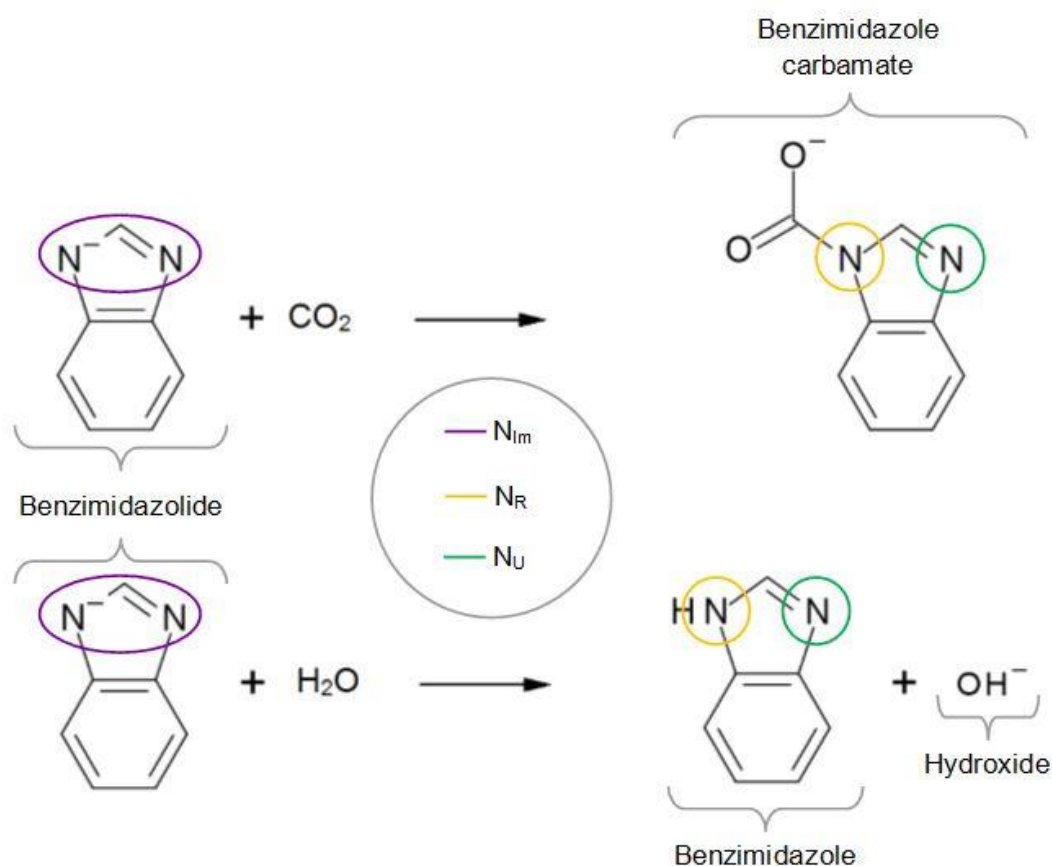
Scheme 2. Proposed reaction between a benzimidazolide ([benzim]⁻) anion and CO_2 (top), generating a carbamate group bound to the previously negatively-charged N, forming benzimidazole carbamate. The proposed reaction between a benzimidazolide anion and H_2O is shown (bottom), where the anion is protonated (forming imidazole) and generates a hydroxide

anion. The violet circles highlight the imidazolide N (labelled N_{Im}), the amber circles highlight the reacted N of both the carbamate and imidazole (labelled N_R), and the green circles highlight the unreacted N of both reactions (labelled N_U).

When the IL is exposed to only 2 mbar H_2O (Stage 6), the N_U and N_R peaks both decrease in intensity. This further supports the theory that the IL can be regenerated through a reduction in surrounding CO_2 partial pressure. The intensities of these peaks, however, do not completely return to the same values as those from the regenerated IL, confirming that there is an interaction between the IL and H_2O vapor. Since the N_U and N_R peaks are much less intense when only exposed to H_2O, this seems to indicate a preferential reaction with CO_2 over H_2O. During the second mixed-gas regime (Stage 7), when the IL is exposed to 2 mbar H_2O and 3 mbar CO_2 once again, the N_U and N_R peaks increase in intensity, with similar peak area ratios as those in Stage 5. From the assignments above one would expect that the N_R and N_U peaks should have a roughly equal intensity.
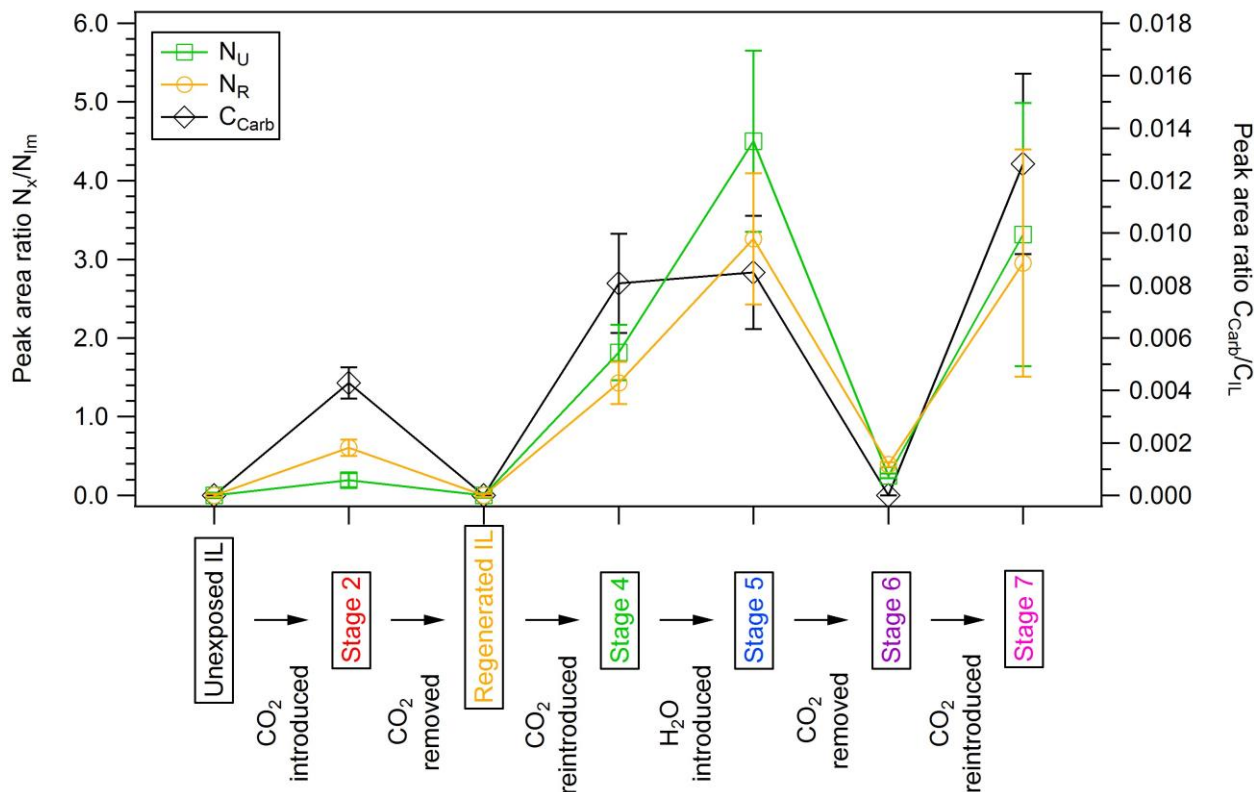
Figure 5. Displayed on the left axis: peak area ratios of N_U/N_{Im} (green squares) and N_R/N_{Im} (amber circles), where N_U refers to unreacted nitrogen, NR refers to reacted nitrogen, and N_{Im} refers to imidazolide nitrogen. Displayed on the right axis: the peak area ratio of C_{Carb}/C_{IL} (black diamonds), where C_{Carb} refers to carbamate carbon, and C_{IL} refers to IL carbon.

Figure 5 shows the peak area ratios of N_U/N_{Im} and N_R/N_{Im} for each stage of experiment. The peak area ratios were calculated by dividing the area of the N_U or N_R peak by the area of the N_{Im} peak at each stage. The N_U and N_R peaks in the N 1s spectra for the unexposed IL and the regenerated IL have been accounted for in the calculations for the ratios calculated for Stages 2, and Stages 4 to 7. Specifically, the areas of the N_U and N_R peaks from the unexposed IL and the regenerated IL have been subtracted from the areas of the N_U and N_R peaks from later stages. Through Stages 3 to 7, it can be seen that $N_U/N_{Im} > N_R/N_{Im}$. This means the area of the N_U peak

is consistently greater than that of N_R throughout these stages, which means a peak area ratio of 1:1 is not maintained. The reasons for this are unclear. One possibility is that some of the absorbed CO_2, rather than forming a carbamate group, weakly interacts with the benzimidazolide anion, causing a shift in the imidazolide N peak to a higher BE. This could account for the consistently greater intensity of N_U compared to N_R, since increased gas exposure would lead to more CO_2 absorption (via both physisorption and chemisorption) and a greater number of these weak interactions between the anion and CO_2 molecules. It is possible that X-ray beam damage occurs, although this is usually indicated by the presence of a feature at low binding energy (~ 397 eV)[16]. From the data here, it is not possible to unambiguously identify the origin of this apparent discrepancy. Further work utilizing angle resolved photoemission, (to vary the depth) and near edge X-ray absorption fine structure may prove useful in elucidating the source of the increased intensity. The peak area ratio C_{Carb}/C_{IL} at each stage of the experiment is shown on the right axis of Figure 5. The C 1s peak intensities are normalized to the IL carbon peak, allowing for comparison of changes in the carbamate carbon peak intensity throughout the experiment. This ratio describes the change in intensity of the carbamate signal only, while both of the ratios of N_U/N_{Im} and N_R/N_{Im} describe intensity changes associated with both carbamate formation and benzimidazole formation. C_{Carb}/C_{IL} does not increase as significantly as N_U/N_{Im} or N_R/N_{Im} when the IL is exposed to H_2O in the first mixed gas regime (Stage 5). This confirms that the increase in N_U and N_R from Stage 4 to Stage 5 is largely due to the reaction with water. C_{Carb}/C_{IL} decreases significantly when the IL is exposed to only H_2O (Stage 6), which reflects the trend displayed by both N_U/N_{Im} and N_R/N_{Im}. Once the IL is exposed to the second mixed-gas regime (Stage 7), C_{Carb}/C_{IL} increases, again reflecting the trend displayed by both N_U/N_{Im} and N_R/N_{Im}.

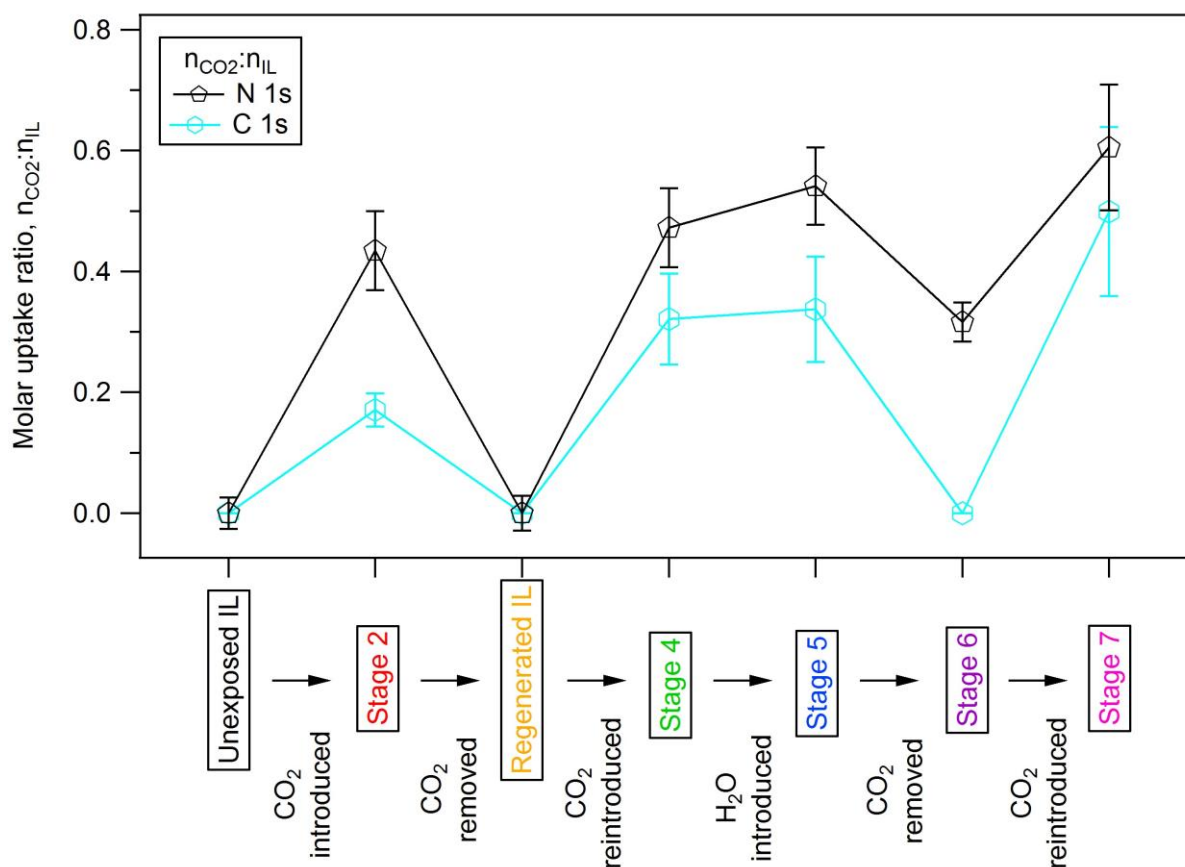This supports the idea that the IL continues to react with CO_2 despite initially exposing the IL to H_2O vapor.

Figure 6. Molar uptake ratio, n_{CO2}:n_{IL}, at each stage of the experiment, calculated using the N 1s region (black pentagons) and the C 1s region (cyan hexagons).

The molar uptake ratio, n_{CO2}:n_{IL} was calculated using the area of the N_R peak in the N 1s region, and the area of the whole N 1s region. For comparison, a separate value for the molar uptake ratio was calculated using the area of the carbamate peak and the area of the whole C 1s region (excluding gas-phase signals). Similarly to the N 1s area ratios, the N_U and N_R peaks from the unexposed IL and regenerated IL have been accounted for in the calculation of the molar

uptake ratio at each Stage. These values of n_{CO2}:n_{IL} at each stage have been plotted in Figure 6. In the study by Taylor et al[6], they calculated the molar uptake ratio of CO_2 in dry [P_{66614}][benzim] (at saturation) to be 1.2. It is likely to be the case that the chemisorption of CO_2 occurs 1:1, but can exceed capacity by 'trapping' physisorbed CO_2. It was found the addition of water reduced the molar uptake ratio of CO_2 to 1, which indicates saturation of the IL with water diminishes its capacity for physisorbed CO_2. Throughout all stages of the experiment the ratio n_{CO2}:n_{IL} is always <1 which is expected since the imidazolide signal is always present in the N 1s region, and therefore some unreacted anions remain in the IL. The molar uptake ratio calculated using these regions follow a similar trend, but n_{CO2}:n_{IL} for the C 1s region is always less than that calculated using the N 1s region at every stage. There are two reasons for this. Firstly, the reaction with H_2O leads to an increase in the intensity of the N_R peak. As a result, the molar uptake ratio calculated using the N 1s region is overestimated. Secondly, the presence of any contaminant C at the surface, likely as a part of silicon grease (see SI), has not been taken into account[37-38]. The signal would overlap with that of the IL, and so would contribute to the intensity of the IL carbon peak. This intensity inflation consequently reduces the apparent relative intensity of the carbamate peak, causing the molar uptake ratio calculated using the C 1s region to be underestimated. This would have a similar effect on the peak area ratio, C_{Carb}/C_{IL}, where the intensity inflation leads to a decrease in the ratio.

The values of n_{CO2}:n_{IL} calculated using the N 1s region averages at ~0.5, irrespective of CO_2 partial pressure. A consistent uptake ratio may be explained by the existence of a threshold of 'surface saturation', where reacted species move to the bulk of the IL, and a portion of unreacted species are present at the surface. An XPS investigation into the reaction between a solution of MEA and CO_2 by Lewis *et al.*[39] demonstrated that the concentration of reacted species was

greater in the bulk of the solution, whereas the concentration of the unreacted MEA was greater at the surface. The IL film studied here is greater than the sampling depth of XPS (see SI), and is therefore considered a bulk system. It may be the case for $[P_{66614}][benzim]$ that the anions that have reacted with CO_2 move to the bulk of the IL, and unreacted anions become more prevalent at the surface of the IL. If a portion of unreacted species consistently populates the IL/CO_2 interface, this would facilitate continuous reaction between the IL and CO_2 until saturation. However, $[P_{66614}][benzim]$ is significantly more viscous than MEA[6, 40-41], which is likely to hinder transport of reacted species in the IL. In previous studies, the IL was subject to saturation of CO_2/H_2O[6], but at these pressures, we are predominantly investigating absorption phenomena via chemisorption due to changes in the N 1s following reaction between CO_2 and the IL. While physisorption of CO_2 cannot be ruled out, the C 1s and O 1s spectra recorded in this work cannot be deconvoluted sufficiently to determine the presence of physisorbed or absorbed CO_2.

It is evident from the signals attributed to carbamate formation in both the C 1s and N 1s regions that IL continues to react with CO_2, irrespective of whether it is exposed to CO_2 or H_2O vapor first. This demonstrates that its ability to react is not significantly inhibited by exposure to H_2O vapor. As mentioned previously, in the study by Taylor et al[6], the capacity for chemisorbed CO_2 was maintained (i.e. 1:1 ratio of CO_2 molecules to IL pairs), but the capacity for physisorbed CO_2 ('trapped' CO_2, the remaining 0.2 of the dry IL molar uptake ratio) was reduced. This is also reflected in our data, whereby the molar uptake ratio (which is likely to be dominated by chemisorption) is a similar value in both mixed-gas regimes, demonstrating that the capacity for chemisorption, under these conditions, was not significantly affected by initial exposure to H_2O vapor. The peak area ratios N_U/N_{Im}, N_R/N_{Im}, and C_{Carb}/C_{IL} in the second mixed-gas regime (Stage 7) are consistent with those in the first mixed-gas regime (Stage 5). This

23

means that the IL reacts with CO_2 and forms a similar proportion of carbamate groups irrespective of whether the IL has been exposed initially to H_2O vapor or CO_2 gas. The idea that a similar number of carbamate groups formed in Stages 5 and 7 suggests that H_2O does not displace CO_2, but CO_2 molecules do displace the hydrogen bonds formed via the reaction between the IL and H_2O.

In previous work,[6] the superbasic ILs were regenerated through heating to 80°C, and removing the desorbed CO_2 under a flow of N_2 [6]. The measurements discussed here have shown that $[P_{66614}][benzim]$ can be regenerated by reducing the CO_2 partial pressure surrounding it. This might also suggest that when working at such low pressures (compared to those employed by Taylor *et al.*) the IL is more easily deprotonated allowing the reaction with CO_2 to proceed. The measurements here clearly demonstrate that the CO_2 capture capabilities of superbasic ILs are not diminished after regeneration for both dry and pre-wetted superbasic ILs.

CONCLUSION

In summary, the reaction of CO_2 with $[P_{66614}][benzim]$ has been studied by NAPXPS and indicates reaction between the CO_2 and benzimidazolide N atoms to form a carbamate species. The results obtained during exposure to both H_2O vapor and CO_2 indicate that the ability of the IL to react with CO_2 is not inhibited significantly by the presence of H_2O, and that CO_2 appears to preferentially bind to the IL, even after exposure to H_2O vapor. The upper limit of the molar uptake ratio, $n_{CO2}:n_{IL}$, is calculated to be approximately 0.5. Additionally, the CO_2 reaction with the anion appears to be reversible simply by reducing the surrounding CO_2 pressure, showing that $[P_{66614}][benzim]$ can be regenerated in situ.

ASSOCIATED CONTENT

Supporting Information. X-ray photoelectron spectra (survey, C 1s, O 1s, N 1s, P 2p) under ultra-high vacuum conditions at normal and grazing emission, and *in situ* X-ray photoelectron spectra of the P 2p region.

AUTHOR INFORMATION

Corresponding Authors

*E-mail: ksyres@uclan.ac.uk; andrew.g.thomas@manchester.ac.uk

Notes

The authors declare no competing financial interests.

Present Addresses

$^{\perp}$ M. W.: DESY, Notkestraße 85, 22607 Hamburg, Germany.

ABBREVIATIONS

[P_{66614}][benzim], trihexyl-tetradecylphosphonium benzimidazolide;

MEA, monoethanolamine;

NAPXPS, near-ambient pressure X-ray photoelectron spectroscopy;

REFERENCES

1.   Haszeldine, R. S., Carbon capture and storage: how green can black be? *Science* **2009,** *325* (5948), 1647-1652.

2.   MacDowell, N.; Florin, N.; Buchard, A.; Hallett, J.; Galindo, A.; Jackson, G.; Adjiman, C. S.; Williams, C. K.; Shah, N.; Fennell, P., An overview of CO2 capture technologies. *Energy & Environmental Science* **2010,** *3* (11), 1645-1669.

3.   Yu, K. M. K.; Curcic, I.; Gabriel, J.; Tsang, S. C. E., Recent advances in CO2 capture and utilization. *ChemSusChem* **2008,** *1* (11), 893-899.

4.   Tenney, S. A.; Lu, D.; He, F.; Levy, N.; Perera, U. G. E.; Starr, D. E.; Müller, K.; Bluhm, H.; Sutter, P., Key structure–property relationships in CO2 capture by supported alkanolamines. *The Journal of Physical Chemistry C* **2014,** *118* (33), 19252-19258.

5.   Rochelle, G. T., Amine scrubbing for CO2 capture. *Science* **2009,** *325* (5948), 1652-1654.

6.   Taylor, S. F. R.; McCrellis, C.; McStay, C.; Jacquemin, J.; Hardacre, C.; Mercy, M.; Bell, R. G.; de Leeuw, N. H., CO2 capture in wet and dry superbase ionic liquids. *Journal of Solution Chemistry* **2015,** *44* (3), 511-527.

7.   Blanchard, L. A.; Hancu, D.; Beckman, E. J.; Brennecke, J. F., Green processing using ionic liquids and CO2. *Nature* **1999,** *399* (6731), 28-29.

8.   Niedermaier, I.; Bahlmann, M.; Papp, C.; Kolbeck, C.; Wei, W.; Krick Calderón, S.; Grabau, M.; Schulz, P. S.; Wasserscheid, P.; Steinrück, H.-P., Carbon dioxide capture by an amine functionalized ionic liquid: fundamental differences of surface and bulk behavior. *Journal of the American Chemical Society* **2013,** *136* (1), 436-441.

9.   Goodrich, B. F.; de la Fuente, J. C.; Gurkan, B. E.; Lopez, Z. K.; Price, E. A.; Huang, Y.; Brennecke, J. F., Effect of water and temperature on absorption of CO2 by amine-functionalized anion-tethered ionic liquids. *The Journal of Physical Chemistry B* **2011,** *115* (29), 9140-9150.

10.   Stevanovic, S.; Podgorsek, A.; Moura, L.; Santini, C.; Padua, A. A.; Gomes, M. C., Absorption of carbon dioxide by ionic liquids with carboxylate anions. *International Journal of Greenhouse Gas Control* **2013,** *17*, 78-88.

11.   Wang, C.; Luo, H.; Li, H.; Zhu, X.; Yu, B.; Dai, S., Tuning the physicochemical properties of diverse phenolic ionic liquids for equimolar CO2 capture by the substituent on the anion. *Chemistry–A European Journal* **2012,** *18* (7), 2153-2160.

12.   Mercy, M.; Rebecca Taylor, S. F.; Jacquemin, J.; Hardacre, C.; Bell, R. G.; De Leeuw, N. H., The addition of CO2 to four superbase ionic liquids: a DFT study. *Physical Chemistry Chemical Physics* **2015,** *17* (43), 28674-28682.

13.   Reinert, F.; Hüfner, S., Photoemission spectroscopy—from early days to recent applications. *New Journal of Physics* **2005,** *7* (1), 97.

14.   Damascelli, A., Probing the electronic structure of complex systems by ARPES. *Physica Scripta* **2004,** *2004* (T109), 61-74.

15.   Lockett, V.; Sedev, R.; Bassell, C.; Ralston, J., Angle-resolved X-ray photoelectron spectroscopy of the surface of imidazolium ionic liquids. *Physical Chemistry Chemical Physics* **2008,** *10* (9), 1330-1335.

16.   Lovelock, K. R. J.; Smith, E. F.; Deyko, A.; Villar-Garcia, I. J.; Licence, P.; Jones, R. G., Water adsorption on a liquid surface. *Chem. Commun.* **2007,** (46), 4866-4868.

17.   Villar-Garcia, I. J.; Smith, E. F.; Taylor, A. W.; Qiu, F. L.; Lovelock, K. R. J.; Jones, R. G.; Licence, P., Charging of ionic liquid surfaces under X-ray irradiation: the measurement of absolute binding energies by XPS. *Physical Chemistry Chemical Physics* **2011,** *13* (7), 2797-2808.

18.   Wagstaffe, M.; Jackman, M. J.; Syres, K. L.; Generalov, A.; Thomas, A. G., Ionic liquid ordering at an oxide surface. *ChemPhysChem* **2016,** *17* (21), 3430-3434.

19.   Syres, K. L.; Jones, R. G., Adsorption, desorption, and reaction of 1-octyl-3-methylimidazolium tetrafluoroborate,[C8C1Im][BF4], ionic liquid multilayers on Cu (111). *Langmuir* **2015,** *31* (36), 9799-9808.

20.   Rivera-Rubero, S.; Baldelli, S., Influence of water on the surface of the water-miscible ionic liquid 1-butyl-3-methylimidazolium tetrafluoroborate: a sum frequency generation analysis. *The Journal of Physical Chemistry B* **2006,** *110* (31), 15499-15505.

21.   Jackman, M. J.; Thomas, A. G.; Muryn, C., Photoelectron spectroscopy study of stoichiometric and reduced anatase TiO2(101) surfaces: the effect of subsurface defects on water adsorption at near-ambient pressures. *The Journal of Physical Chemistry C* **2015,** *119* (24), 13682–13690.

22.   Starr, D. E.; Liu, Z.; Havecker, M.; Knop-Gericke, A.; Bluhm, H., Investigation of solid/vapor interfaces using ambient pressure X-ray photoelectron spectroscopy. *Chemical Society Reviews* **2013,** *42* (13), 5833-5857.

23.   Stoerzinger, K. A.; Hong, W. T.; Crumlin, E. J.; Bluhm, H.; Shao-Horn, Y., Insights into electrochemical reactions from ambient pressure photoelectron spectroscopy. *Accounts of Chemical Research* **2015,** *48* (11), 2976-2983.

24.   Henderson, Z.; Walton, A. S.; Thomas, A. G.; Syres, K. L., Water-induced reordering in ultrathin ionic liquid films. *Journal of Physics: Condensed Matter* **2018,** *30* (33), 334003.

25.   Broderick, A.; Khalifa, Y.; Shiflett, M. B.; Newberg, J. T., Water at the ionic liquid–gas interface examined by ambient pressure X-ray photoelectron spectroscopy. *The Journal of Physical Chemistry C* **2017,** *121* (13), 7337-7343.

26.   Khalifa, Y.; Broderick, A.; Newberg, J. T., Water vapor electron scattering cross-section measurements using a hydrophobic ionic liquid. *Journal of Electron Spectroscopy and Related Phenomena* **2018,** *222*, 162-166.

27.   Khalifa, Y.; Broderick, A.; Newberg, J. T., Surface enhancement of water at the ionic liquid–gas interface of [HMIM][Cl] under ambient water vapor. *Journal of Physics: Condensed Matter* **2018,** *30* (32), 325001.

28.   Blundell, R. K.; Licence, P., Quaternary ammonium and phosphonium based ionic liquids: a comparison of common anions. *Physical Chemistry Chemical Physics* **2014,** *16* (29), 15278-15288.

29.   Fairley, N., *CasaXPS Manual 2.3.15 Introduction to XPS and AES*. Casa Software: 2009.

30.   Bezerra, D. P.; da Silva, F. W.; de Moura, P. A.; Sousa, A. G.; Vieira, R. S.; Rodriguez-Castellon, E.; Azevedo, D. C., CO2 adsorption in amine-grafted zeolite 13X. *Applied Surface Science* **2014,** *314*, 314-321.

31.   Eren, B.; Heine, C.; Bluhm, H.; Somorjai, G. A.; Salmeron, M., Catalyst chemical state during CO oxidation reaction on Cu (111) studied with ambient-pressure X-ray photoelectron spectroscopy and near edge X-ray adsorption fine structure spectroscopy. *Journal of the American Chemical Society* **2015,** *137* (34), 11186-11190.

32.   Walle, L.; Borg, A.; Uvdal, P.; Sandell, A., Probing the influence from residual Ti interstitials on water adsorption on TiO 2 (110). *Physical Review B* **2012,** *86* (20), 205415.

33.   Ketteler, G.; Yamamoto, S.; Bluhm, H.; Andersson, K.; Starr, D. E.; Ogletree, D. F.; Ogasawara, H.; Nilsson, A.; Salmeron, M., The nature of water nucleation sites on TiO2 (110) surfaces revealed by ambient pressure X-ray photoelectron spectroscopy. *The Journal of Physical Chemistry C* **2007,** *111* (23), 8278-8282.

34.   Seyller, T.; Borgmann, D.; Wedler, G., Interaction of CO2 with Cs-promoted Fe (110) as compared to Fe (110)/K+ CO2. *Surface science* **1998,** *400* (1-3), 63-79.

35.   Thompson, R. L.; Shi, W.; Albenze, E.; Kusuma, V. A.; Hopkinson, D.; Damodaran, K.; Lee, A. S.; Kitchin, J. R.; Luebke, D. R.; Nulwala, H., Probing the effect of electron donation on CO2 absorbing 1, 2, 3-triazolide ionic liquids. *RSC Advances* **2014,** *4* (25), 12748-12755.

36.   Morales-Gil, P.; Walczak, M.; Cottis, R.; Romero, J.; Lindsay, R., Corrosion inhibitor binding in an acidic medium: Interaction of 2-mercaptobenizmidazole with carbon-steel in hydrochloric acid. *Corrosion Science* **2014,** *85*, 109-114.

37.   Hashimoto, H.; Ohno, A.; Nakajima, K.; Suzuki, M.; Tsuji, H.; Kimura, K., Surface characterization of imidazolium ionic liquids by high-resolution Rutherford backscattering spectroscopy and X-ray photoelectron spectroscopy. *Surface Science* **2010,** *604* (3), 464-469.

38.   Smith, E. F.; Rutten, F. J.; Villar-Garcia, I. J.; Briggs, D.; Licence, P., Ionic liquids in vacuo: analysis of liquid surfaces using ultra-high-vacuum techniques. *Langmuir* **2006,** *22* (22), 9386-9392.

39.   Lewis, T.; Faubel, M.; Winter, B.; Hemminger, J. C., CO2 capture in amine-based aqueous solution: role of the gas–solution interface. *Angewandte Chemie International Edition* **2011,** *50* (43), 10178-10181.

40.   DiGuilio, R. M.; Lee, R. J.; Schaeffer, S. T.; Brasher, L. L.; Teja, A. S., Densities and viscosities of the ethanolamines. *Journal of Chemical and Engineering Data* **1992,** *37* (2), 239-242.

41.   Maham, Y.; Liew, C.-N.; Mather, A., Viscosities and excess properties of aqueous solutions of ethanolamines from 25 to 80 C. *Journal of Solution Chemistry* **2002,** *31* (9), 743-756.

TOC GRAPHIC